A transistor-only power-efficient high-frequency voltage-mode stimulator for a multichannel system

Marijn N. van Dongen and Wouter A. Serdijn
Biomedical Electronics Laboratory, Delft University of Technology, The Netherlands
Email: M.N.vanDongen@tudelft.nl

***Abstract*—This paper proposes a fully implantable high-frequency switched-mode neural stimulator. The main circuit consists of 2N transistors for an N-electrode system in which all channels can be stimulated concurrently and independently. System simulations show that power efficiencies of 80% or higher are feasible over the full output range.**

The system is powered from a single-ended battery voltage and does not need external components. It uses the dynamic properties of neurons to filter the high-frequency signal such that the resulting stimulation becomes equivalent to that of traditional stimulation.

The system has a voltage-mode output and therefore safety aspects such as charge cancellation are carefully considered. Also the influence of high-frequency mode operation is considered as far as available models allow.

Using system-level simulations the functionality of the system is illustrated from circuit level down to axon level. Furthermore a discrete-component prototype is constructed to verify that the stimulation protocol is able to successfully induce activation in the tissue.

I. Introduction

The power consumption of the output stage is an important factor in the power budget of implantable neural stimulators. Therefore the power efficiency of this stage is of major concern in the design. Most existing designs employ a linear output stage, yielding low power efficiency if the output voltage is low compared to the supply voltage.

Several attempts have been proposed to increase the power efficiency. The supply voltage can be made variable using a compliance monitor (class H operation) [1]. Also switched-mode operation has been proposed to increase the power efficiency [2].

In [3] a high frequency switched-mode stimulation scheme was proposed that utilizes the tissue properties to achieve efficient stimulation with a minimum number of external components. One external inductor is used to achieve a current-mode output at an output voltage level that can be higher or lower than the battery voltage.

Current-mode output is not a necessity for effective stimulation. If furthermore a high enough supply voltage is available (for example if the electrode impedance is relatively low), it is possible to apply stimulation without the use of an external inductor. In this paper an energy efficient fully implantable high frequency voltage-mode stimulator circuit is proposed without the need of external components. The system also supports multichannel operation.

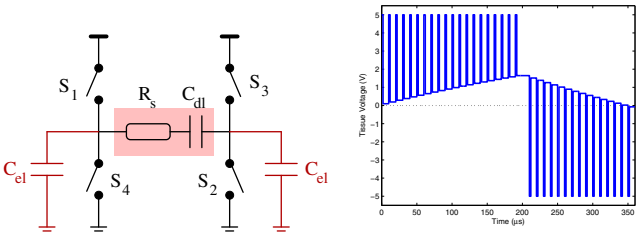

(a) System with parasitics (b) Full stimulation cycle

Fig. 1. System design a) of the proposed stimulator system ($S_1 - S_4$) with the parasitic capacitors C_{el} as well as the tissue model consisting of R_s and C_{dl}. In b) a system level simulation of V_{stim} during a biphasic stimulation cycle is shown

II. System design

The system design is depicted in Figure 1a. The circuit basically consists of an H-bridge (to control the direction of stimulation signal V_{stim}) that is connected to the supply voltage directly. By means of Pulse Width Modulation (PWM) the average voltage V_{avg} over the tissue is controlled. The simplest model for the tissue is an RC series circuit. In this model the capacitance C_{dl} represents the electrode-tissue interface and the resistor R_s represents the tissue impedance.

During the first stimulation phase Switch S_2 is closed, while switch S_1 is periodically opened and closed using PWM. During the second stimulation phase the current direction is reversed by closing switch S_4 and enabling S_3 with PWM. An overview of the voltage across the tissue during a stimulation phase is given in Figure 1b. A constant duty cycle $\delta = 0.2$ is chosen in this example. Together with a supply voltage of $V_{dd} = 5\,\mathrm{V}$ this results in $V_{avg} = \delta V_{dd} = 1\,\mathrm{V}$. The tissue model has been dimensioned as $R_s = 2\,\mathrm{k\Omega}$ and $C_{dl} = 50\,\mathrm{nF}$.

The duty cycle δ can effectively increase or decrease the stimulation intensity V_{avg}. Note that the absolute amount of charge injected depends on the tissue impedance as well. To increase or decrease the neural response a relative increase and decrease using δ is sufficient, but charge control is important when considering charge cancellation. Charge cancellation is considered in Section IVB. Here the pulsewidth of the second pulse has been adjusted to approximate charge cancellation.

The frequency of the PWM signal should be chosen such that an output filter can block the high frequency switching components and only V_{avg} remains. Similar to the technique described in [3], the properties of the tissue itself will be used

978-1-4799-1471-5/13/$31.00 ©2013 IEEE

to filter the stimulation signal without using additional external filter components. In the next section it will be seen that based on these properties a frequency of $f_{sw} = 200\,\text{kHz}$ was chosen.

Note that the system supports multichannel operation. It is possible to connect multiple channels in parallel to the same supply voltage V_{dd}. Since each channel can have its own duty cycle, the channels can be stimulated independently from each other. Each electrode has a total of 2 switches, yielding just $2N$ switches for a N-electrode system. There are limits to the operation of the system in multichannel mode. It is for example not possible to stimulate in two different directions (anodic and cathodic) at two electrodes when they share the same return electrode.

A. *Power efficiency*

The power efficiency of the system depends on the resistive losses and capacitive losses of the H-bridge. The resistive losses depend on the ratio between the on-resistance of the switches R_{on} and the load impedance. If it is assumed that at the end of a stimulation cycle the voltage over C_{dl} is brought back to 0 V, the netto power is divided between R_s and R_{on}:

$$\eta_R = \frac{I_{stim}^2 R_s}{I_{stim}^2 R_s + I_{stim}^2 2R_{on}} = \frac{R_s}{R_s + 2R_{on}} \tag{1}$$

The capacitive losses mainly occur at two locations: the parasitic capacitance at the gates of the switches and the parasitic capacitance at the electrodes. When only considering the gate capacitance C_{gate} of the switches with the PWM signal, the losses are given by:

$$\eta_{C_{gate}} = \frac{\delta}{\delta + C_{gate} f_{sw} R_s} \tag{2}$$

This equation assumes that the gates are switched from 0 to V_{dd}. When also incorporating the losses due to the parasitic capacitance at the tissue (C_{el} in Figure 1a), the equation becomes slightly more complicated, because the voltage swing over these capacitance varies as C_{dl} is charged during a stimulation phase. Assuming this effect can be neglected, the electrode capacitance C_{el} can be incorporated as follows:

$$\eta_C = \frac{\delta - C_{el} f_{sw} R_s}{\delta + C_{gate} f_{sw} R_s} \tag{3}$$

When implementing the switches, a tradeoff needs to be made between low R_{on} and acceptable parasitic capacitance depending on the switching frequency and the tissue impedance. The parasitics of a High Voltage (20V) transistor in AMS 0.18μm technology are $R_{on,M} = 1.416\,\text{k}\Omega/M$ and $C_{gate,M} = M111\,\text{fF}$ with M the multiplication factor determining the size of the transistor. Furthermore assuming a constant $C_{el} = 10\,\text{pF}$ due to the bondpads, an estimation can be made for the efficiency using system simulations. The results are depicted in Figure 2 for two different loads and various values of δ, $f_{sw} = 200\,\text{kHz}$ and a pulsewidth of 200 μs. As can be seen it can be expected that with proper transistor dimensioning, efficiencies well above 80% are possible for these settings.

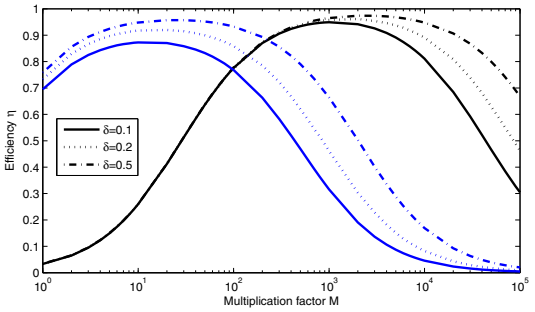

Fig. 2. System simulations of the power efficiency incorporating R_{on}, C_{gate} and C_{el} for various switch dimensions M. The blue line corresponds with a high impedance load ($R_s = 10\,\text{k}\Omega$, $C_{dl} = 10\,\text{nF}$), the black lines with a low impedance ($R_s = 100\,\Omega$, $C_{dl} = 1\,\mu\text{F}$)

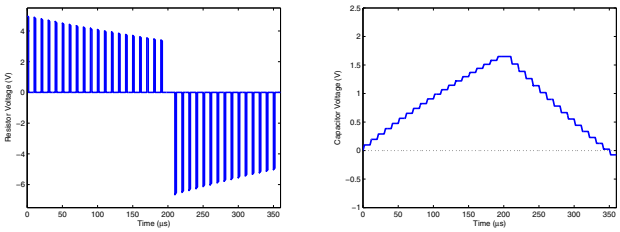

(a) Resistor voltage (b) Capacitor voltage

Fig. 3. Voltage over R_s and C_{dl} during during the stimulation cycle of Figure 1b

III. Using the tissue properties

In Figure 3a the voltage over R_s is plotted during the stimulation cycle of Figure 1b. This voltage is proportional to the strength of the electric field in the tissue. Hence, the electric field will have a pulsating shape. It can now be investigated how this field influences the membrane voltage.

For simplicity the tissue is assumed to have linear homogeneous properties and the electrode is considered to behave like a point source, which is located at the origin. Under these conditions the electric field has a $1/r$ dependence and the voltage at location V(x,y) can be described using [4]:

$$V(x,y) = \frac{\rho_e V_{ext}}{4\pi R_s \sqrt{x^2 + y^2}} \tag{4}$$

Here V_{ext} is the voltage at the electrode. In [4] the activation process is described for an axon under the influence of an electric field. Analogous to [4] a simple myelinated axon model is chosen under subthreshold conditions, which is depicted in Figure 4. In Table I the axon membrane parameters are summarized. This leads for an axon with $d_o = 20\,\mu\text{m}$ to a membrane capacitance $C_m = c_m \pi d_i \nu = 1.41\,\text{pF}$, a subthreshold membrane conductance of $G_m = g_m \pi d_i \nu = 72.4\,\text{nS}$ and an internodal conductance of $G_a = 4\rho_i l / \pi d_i^2 = 103\,\text{nS}$.

Assuming the axon is located at a distance of $d_{axon} = 1\,\text{mm}$ away from the origin and has an orientation as depicted in Figure 4, we can now substitute the waveform of Figure 3a at the voltage sources $V_1 - V_4$ and obtain the membrane voltage as function of the PWM stimulation.

TABLE I
AXON PROPERTIES USED FOR THE SUBTHRESHOLD MODEL [4]

Symbol	Description	Value
ρ_i	axoplasm resistivity	$54.7\,\Omega \cdot \mathrm{cm}$
ρ_o	extracellular resistivity	$0.3\,\mathrm{k}\Omega \cdot \mathrm{cm}$
c_m	nodal membrane capacitance/unit area	$2.5\,\mu\mathrm{F/cm}^2$
g_m	nodal membrane conductance/unit area	$128\,\mathrm{mS/cm}^2$
ν	nodal gap width	$1.5\,\mu\mathrm{m}$
l/d_o	ratio of internode spacing to fiber diameter	100
d_i/d_o	ratio of axon diameter (internal myelin) to fiber diameter	0.6

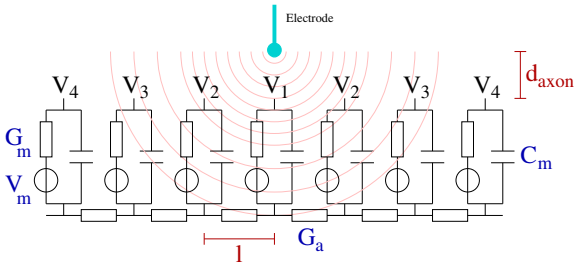

Fig. 4. Axon cable model and its orientation with respect to an electrode modeled as a point source

The result is depicted in Figure 5a. As can be seen, the time constant of the axon membrane filters the PWM signal and the membrane voltage is raised. When the increase is high enough to reach the threshold voltage, it would mean that the PWM signal should be able to induce an action potential in this axon.

The switched-mode response is compared with classic constant current stimulation with the same average intensity of $I_{stim,dc} = V_{avg}/R_s = 500\,\mu\mathrm{A}$. Indeed the response is similar in the sense that in both cases the membrane potential is elevated with the same amount.

From Figure 5a the influence of the charging of capacitor C_{dl} is clearly visible in the switched-mode response: the voltage over R_s is slowly decreasing, causing the electric field to become smaller and thus the axon voltage to reduce. In the case of constant current stimulation this does not happen, since the voltage drop over R_s is constant.

Note that the membrane time constant $\tau_m = C_m/G_m = c_m/g_m = 19.5\mu s$ is independent on the axon diameter. This means that the proposed technique does not depend on the axon size as long as the parameters from Table I are valid. This is illustrated in Figure 5b by showing the axon voltage for three different axon widths: $5\,\mu\mathrm{m}$, $12\,\mu\mathrm{m}$ and $20\,\mu\mathrm{m}$.

IV. SAFETY

There are two safety issues that need to be covered relating to the system architecture proposed here: the influence of the high current, low duty cycle stimulation and charge cancellation. Both issues will be discussed in the next sections.

A. High current, low duty cycle

For low duty cycles, V_{stim} has relatively high peak amplitudes (V_{avg}/V_{dd} is relatively low). Since classic stimulation schemes do not use this, the related safety aspects are investigated.

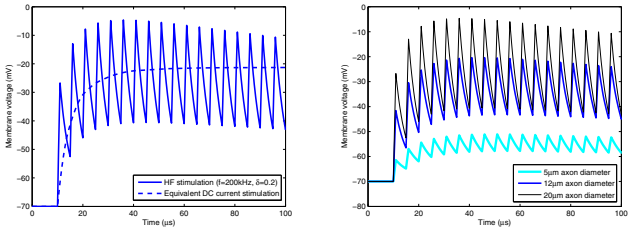

(a) Axon with = $20\,\mu\mathrm{m}$ (b) Various widths

Fig. 5. Membrane voltage of an axon stimulated by an electric field with the shape depicted in Figure 3a.

One of the damage mechanisms during neural stimulation is due to electrochemical reactions. In Figure 3b the voltage over C_{dl} is plotted during a stimulation phase. This voltage is directly related to the amount of electrochemical reactions I_r during a stimulation phase via the Butler-Volmer equation [5]:

$$I_f = I_s * [\exp(-nRF\alpha\eta) + \exp(-nRF(1-\alpha)\eta)] \quad (5)$$

Here η repesents the voltage over capacitor C_{dl}. From Figure 3b it is seen that the swing over this capacitor is the same as for classical stimulation, since the average energy injected through the interface is the same. Therefore in terms of electrochemical reactions, no difference is expected.

Tissue can also be damaged due to other effects. The available empirical models for tissue damage due to stimulation [6], [7] are largely based on charge density and charge per phase. They are not considering the high frequency behavior of the proposed system and can therefore not easily predict whether this system would lead to damage or not. More research is needed in order to investigate this.

One way of reducing the peak amplitude is by providing multiple voltage levels, for example by incorporating power efficient DC-DC converters in the system. In this way the minimum duty cycle required can be increased. However, such efficient DC-DC converters typically need one or more external passive components.

B. Charge cancellation

Since the proposed system has a voltage steered characteristic, the issue of charge cancellation needs to be addressed. The voltage of C_{dl} is not allowed to accumulate over time in order to prevent harmful electrochemical reactions [8].

It is possible to use a dynamic algorithm that adjusts the pulse width of the charge cancelation pulse based on the resulting voltage over the tissue V_{rest} after a stimulation pulse [9]. After a stimulation cycle the pulsewidth of the second pulse during the next stimulation cycle is increased or decreased based on the value of V_{rest}. Since a high frequency system is used, it is easy to control the pulse width by controling the number of pulses injected.

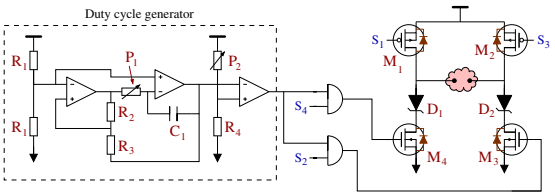

Fig. 6. Circuit design of the prototype. A variable duty cycle generator is used to create a PWM signal for the NMOS transistors.

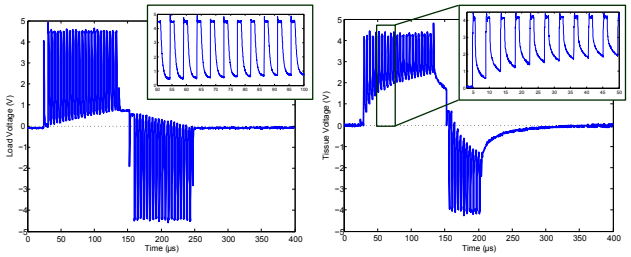

(a) $R_s = 5.6\,\mathrm{k}\Omega$, $C_{dl} = 39\,\mathrm{nF}$ (b) Electrodes in mouth

Fig. 7. Measurement results of the load voltage during a full stimulation cycle. In a) the load is a $R_s = 5.6\,\mathrm{k}\Omega$, $C_{dl} = 39\,\mathrm{nF}$ model, in b) the load is a pair of electrodes placed in the mouth of a subject

V. Prototype

In order to verify whether this stimulation architecture is able to induce activation, a simple prototype was built. The circuit design is depicted in Figure 6. Transistors M_1-M_4 form the H-bridge that is connected to $V_{dd} = 5\,\mathrm{V}$, while diodes D_1 and D_2 are used to prevent leakage through ESD protection diodes in the circuitry whenever the potential at one of the terminals of the interface capacitor has negative values with respect to ground.

The signals S_1-S_4 control the gates of transistors M_1-M_4 respectively. An Arduino Microcontroler platform is used to generate these signals such that the H-bridge is controlled correctly. The PWM signal was generated using a saw-tooth generator in combination with a comparator circuit. Potentiometer P_1 is used to control the frequency (200 kHz was chosen) and P_2 is used to tune δ.

The charge cancellation scheme was implemented using the dynamic algorithm that adjusts the second pulse width based on the voltage remaining over the tissue, which can be measured using the built-in ADC in the Arduino platform.

The circuit is first connected to an RC model with $R_s = 5.6\,\mathrm{k}\Omega$ and $C_{dl} = 39\,\mathrm{nF}$. The measurement results for $\delta = 0.2$ are depicted in Figure 7a and they resemble the system simulations quite well. The charge cancellation scheme causes the second pulse to be shorter, since the current is during this phase is higher (due to a negative voltage over C_{dl}).

The circuit is then connected to percutaneous electrodes (manufactured by St. Jude) with an $R_s \approx 100\,\Omega$ in a saline solution. The electrodes are placed in the mouth of a subject. The measurement results for the same settings are shown in Figure 7b. They are similar to the model, except that C_{dl} is charging in a non linear fashion. This is due to the non linear properties of the electrode-tissue interface.

Most important of all is that the subject was able to feel the stimulation. Also by varying δ the subject could feel a variation of stimulation intensity. This indicates that the proposed algorithm is able to induce effective stimulation and that it can be controlled using δ.

VI. Conclusion

A novel system design for neurostimulator circuits is proposed. It uses PWM operation and uses the tissue properties to filter out the switching effects and establish effective activation of neurons. In this way it eliminates the need for passive components entirely and the circuit consists of just two transistors for each electrode.

Furthermore power efficiency is expected to be high over a large range of stimulation intensities (well above 80%). Other energy efficient systems often use one or more bulky external components for each channel [2].

The simple design makes the system very suitable for multichannel operation in which each channel can be controlled individually. Since each channel uses the same stimulation voltage, the power efficiency does not degrade for multichannel operation, unlike systems that use one central voltage headroom monitor for multiple electrodes [1].

The safety aspects regarding the proposed stimulation protocol are analyzed as far as the available models allow for it. Furthermore experiments with a subject confirmed that effective stimulation is possible. However, both of these aspects need more in-depth research (such as *in vitro* experiments) to confirm the results presented here.

References

[1] K. Sooksood, E. Noorsal, J. Becker, and M. Ortmanns, "A neural stimulator front-end with arbitrary pulse shape, hv compliance and adaptive supply requiring 0.05mm2 in 0.35m hvcmos," in *IEEE International Solid-State Circuits Conference (ISSCC) Digest of Technical Papers*. IEEE, February 2011, pp. 306–308.

[2] S. Arfin and R. Sarpeshkar, "An energy-efficient, adiabatic electrode stimulator with inductive energy recycling and feedback current regulation," *IEEE Transactions on Biomedical Circuits and Systems*, vol. 6, pp. 1–14, 2012.

[3] M. van Dongen and W. Serdijn, "A switched-mode multichannel neural stimulator with a minimum number of external components," in *IEEE ISCAS*, May 2013.

[4] E. Warman, W. Grill, and D. Durand, "Modeling the effects of electric fields on nerve fibres: Determination of excitation thresholds," *IEEE Transactions on Biomedical Engineering*, vol. 39, no. 12, December 1992.

[5] D. Merrill, M. Bikson, and J. Jefferys, "Electrical stimulation of excitable tissue: design of efficacious and safe protocols," *Journal of Neuroscience Methods*, vol. 141, pp. 171–198, 2005.

[6] A. Butterwick, A. Vankov, P. Huie, Y. Freyvert, and D. Palanker, "Tissue damage by pulsed electrical stimulation," *IEEE Transactions on Biomedical Engineering*, vol. 54, no. 12, pp. 2261–2267, December 2007.

[7] R. Shannon, "A model of safe levels for electrical stimulation," *IEEE Transactions on Biomedical Engineering*, vol. 39, no. 4, pp. 424–426, March 1992.

[8] J. Lilly and J. Hughes, "Brief, noninjurious electric waveform for stimulation of the brain," *Science*, vol. 121, pp. 468–469, 1955.

[9] M. Ortmanns, N. Unger, A. Rocke, M. Gehrke, and H. Tietdke, "A 0.1mm2 digitally programmable nerve stimulation pad cell with high voltage capability for a retinal implant," in *IEEE International Solid-State Circuits Conference (ISSCC) Digest of Technical Papers*. IEEE, 2006, pp. 89–98.